

MSEC2016-8583

EFFECT OF PREHEAT ON IMPROVING BENEFICIAL SURFACE RESIDUAL STRESSES DURING INDUCTION HARDENING PROCESS

Zhichao (Charlie) Li, Andrew Freborg, and Lynn Ferguson

DANTE Solutions, Inc.

7261 Engle Road, Suite 105

Cleveland, Ohio, USA

Charlie.Li@Dante-Solutions.com

KEYWORDS

induction hardening, quench hardening, residual stress, phase transformation, preheat.

ABSTRACT

Applications of the induction hardening process have been gradually increasing in the heat treatment industry due to its energy efficiency, process consistency, and clean environment. Compared to traditional furnace heating and liquid quenching processes, induction hardening is more flexible in terms of process control, and it can offer improved part quality. The commonly modified parameters for the process include the inductor power and frequency, heating time, spray quench delay and quench severity, etc. In this study, a single shot induction hardening process of a cylindrical component made of AISI 4340 is modeled using DANTE[®]. It is known that the residual stresses in a hardened steel component have a significant effect on high cycle fatigue performance, with higher magnitudes of surface residual compression leading to improved high cycle fatigue life. Induction hardening of steel components produces surface residual compression due to the martensitic transformation of the hardened surface layer, with a high magnitude of compression preferred for improved performance in general. In this paper, a preheat concept is proposed with the induction hardening process for enhanced surface residual compression in the hardened case. Preheating can be implemented using either furnace or low power induction heating, and both processes are modeled using DANTE to demonstrate its effectiveness. With the help of computer modeling, the reasons for the development of residual stresses in an induction hardened part are described, and how the preheat can be used to improve the magnitude of surface residual compression is explained.

INTRODUCTION

The induction hardening process is more energy efficient because only the component surface is heated and austenitized, as compared with furnace heating and liquid quenching processes where the process is applied to the entire part cross-section. Induction hardening also gives more options for process optimization for improved case depth and residual stress distribution relative to traditional furnace heating and liquid quenching processes [1-3].

Induction hardening processes generate compressive stresses in the hardened case, especially in outer part surfaces, and the compressive stresses have proven to be beneficial for both fatigue performance and wear resistance [4-5].

Stress evolution during steel heat treatment is a highly nonlinear process due to the phase transformations that occur. With phase transformations, the thermal and mechanical properties change, the material volume changes, the internal stresses within individual phases change, and the stresses between different phases also change. Simulation of stresses and deformation is an emerging technology. Besides the variety and complexity of simulation algorithms, stress simulation requires large databases of thermal, metallurgical and mechanical properties of material phases over the entire range of temperatures used during processing.

Both the power and frequency of the inductor have a significant effect on the heat penetration into the part. Lower frequency tends to heat the the part deeper over a longer time duration because the eddy current gradient in the part surface is relatively low. Conversely, a higher frequency heats the shallower surface layer of the part in a shorter time. The temperature distribution in the part is a combined result of both the thermal conduction and induction heating. In some induction hardening processes, both low/medium frequency and high frequency are used together to reach the desired temperature field. Simultaneous dual frequency (SDF) induction

heating is also used in industry [6]. Different from more standard induction heating, SDF induction heating applies two frequencies in the part simultaneously. By using different percentages of the two frequencies, SDF induction heating improves the flexibility of temperature distribution control in a complicated part.

Induction hardening is a transient thermal process. During induction hardening of steel components, the temperature gradient and phase transformations both contribute to the evolution of the internal stresses and part dimensional change. The improvement and development of heat treatment simulation software make it much easier to understand the material response during the heat treatment process, most specifically concerning the generation of internal stresses and deformation. DANTE is a commercially available heat treatment software based on finite element method that was developed to model carburization and conventional quench hardening processes for steel parts [7-8]. While DANTE was not designed to model the physics of induction heating process, DANTE can be used to simulate the temperature field during induction heating by applying the internal heat flux (I^2R) based on the eddy current distribution in the part.

DESCRIPTION OF INDUCTION HARDENING MODEL

Sample Geometry and FEA Model

A cylindrical component with a radius of 50.8 mm is selected for this study, and the geometry and the finite element mesh are shown in Figure 1. Assuming the cylinder has a high length to diameter ratio, and the part is hardened by a single shot process, one slice of the cylinder with 0.5 mm axial thickness is selected for the modeling study. The finite element mesh has 410 nodes, and 204 linear 4-node elements. The model has two layers of nodes: the top layer and the bottom layer. To represent the long cylinder using this thin sliced model, the bottom layer of nodes is constrained in the axial direction, and the top layer of nodes is constrained to move simultaneously in the axial direction.

Phase Transformation Kinetics

The cylinder used in this study is made of 4340 steel. Phase transformation models are required to model the heating and quench hardening processes [9]. The diffusive and martensitic transformation models in DANTE are described in equations (1) and (2) below.

$$\frac{d\Phi_d}{dt} = v_d(T)\Phi_d^{\alpha 1}(1-\Phi_d)^{\beta 1}\Phi_a \quad (1)$$

$$\frac{d\Phi_m}{dT} = v_m(1-\Phi_m)^{\alpha 2}(\Phi_m + \varphi\Phi_d)^{\beta 2}\Phi_a \quad (2)$$

where Φ_d and Φ_m are the volume fractions of individual diffusive phase and martensite transformed from austenite; Φ_a is the volume fraction of austenite; v_d and v_m are the mobilities of transformation; v_d is a function of temperature, and v_m is a constant; $\alpha 1$ and $\beta 1$ are the constants of diffusive transformation; and $\alpha 2$, $\beta 2$ and φ are constants of martensitic

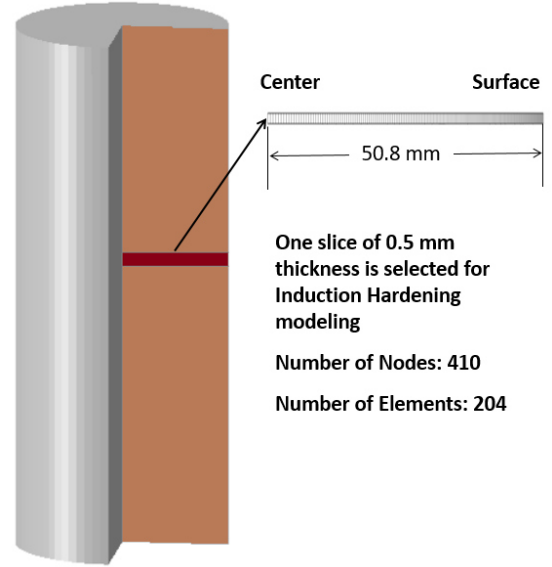


FIGURE 1 – COMPONENT GEOMETRY AND FINITE ELEMENT MODEL.

transformation. For each individual metallurgical phase, one set of transformation kinetics parameters is required.

Figure 2(a) is a continuous cooling dilatometry strain curve generated from the DANTE database representing austenite transformation to martensite for AISI 4340 steel. The horizontal axis in Figure 2(a) is temperature and the vertical axis is strain, so what is not shown is cooling time. The strain change due to martensitic transformation is clearly quantified.

When the dilatometry test sample cools to the martensitic transformation starting temperature (M_s), its volume expands with the crystal structure change from austenite's face centered cubic (FCC) lattice to martensite's body centered tetragonal (BCT) lattice. Martensite's BCT structure has a lower density than austenite's FCC structure. The strain during transformation is a combination of thermal strain, phase transformation volume change, and strain induced by stresses generated during the transformation. The latter strain is referred to as Transformation Induced Plasticity (TRIP). The data obtained from this specific dilatometry test include coefficient of thermal expansion (CTE) for austenite and martensite, martensitic transformation starting and finishing temperature (M_s , M_f), transformation strain, and phase transformation kinetics (transformation rate) from austenite to martensite. These data are critical to the accuracy of modeling the internal stress and deformation caused by quenching.

Diffusive transformations are also characterized by dilatometry tests. A series of dilatometry tests with different cooling rates are required to fit a full set of diffusive and martensitic phase transformation kinetics parameters. Once the full set of phase transformation kinetics parameters are fit from dilatometry tests, isothermal transformation (TTT) and continuous cooling transformation (CCT) diagrams can be generated for users to review. TTT/CCT diagrams are not

directly used by DANTE phase transformation kinetics models, but they are useful because users can see the hardenability of the material graphically. Figure 2(b) is an isothermal transformation diagram (TTT) for 4340 steel created from the DANTE database.

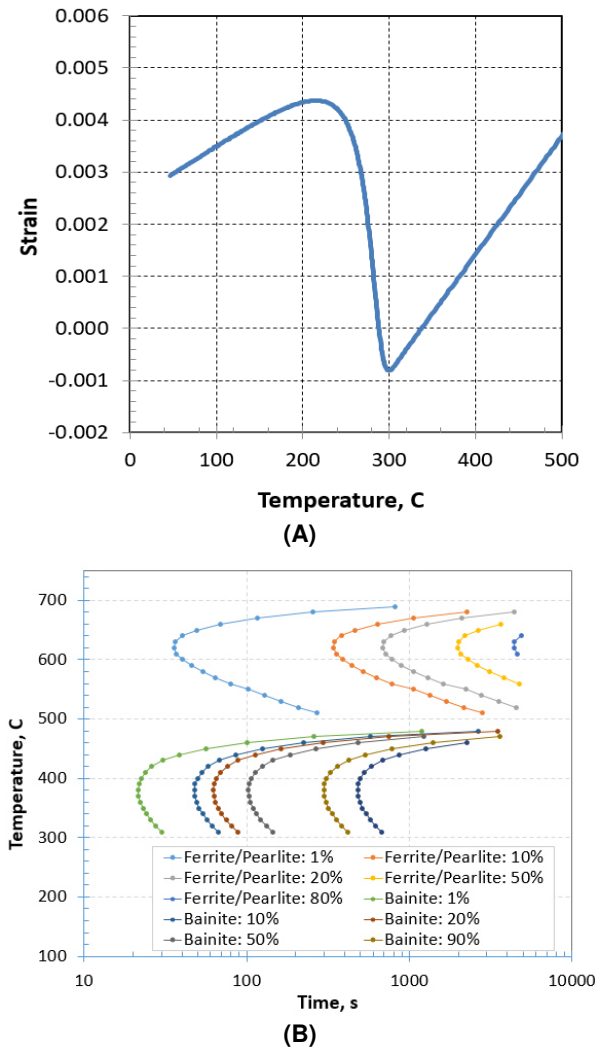


FIGURE 2 – (A) DILATOMETRY STRAIN CURVE DURING CONTINUOUS COOLING, AND (B) TTT DIAGRAMS OF AISI 4340 GENERATED FROM DANTE DATABASE.

BASELINE SINGLE SHOT INDUCTION HARDENING MODEL

Induction Hardening Process Description

The cylinder is heated using a single shot induction heating process. The applied inductor frequency is 3.5 kHz, and the power is 5.0 kW per unit axial length. As shown in Figure 1, the simplified finite element model has an axial length of 0.5 mm, so the power applied in the model is 2.5 kW. The total induction heating time is 7.5 seconds in the baseline model, followed by spray quench immediately without a time delay. A polymer water solution is used as the spray quenching medium,

with the assumption that the heat transfer coefficient is 8,000 W/(m²K), and the quenching medium temperature is 20° C. The total spray quench time is 300 seconds.

Baseline Model Result Analysis

Internal heat generated by the eddy current from the inductor is applied directly to drive the heating model. At the end of the 7 s heating, the temperature distribution in terms of depth from the cylinder outer surface is shown in Figure 3(a).

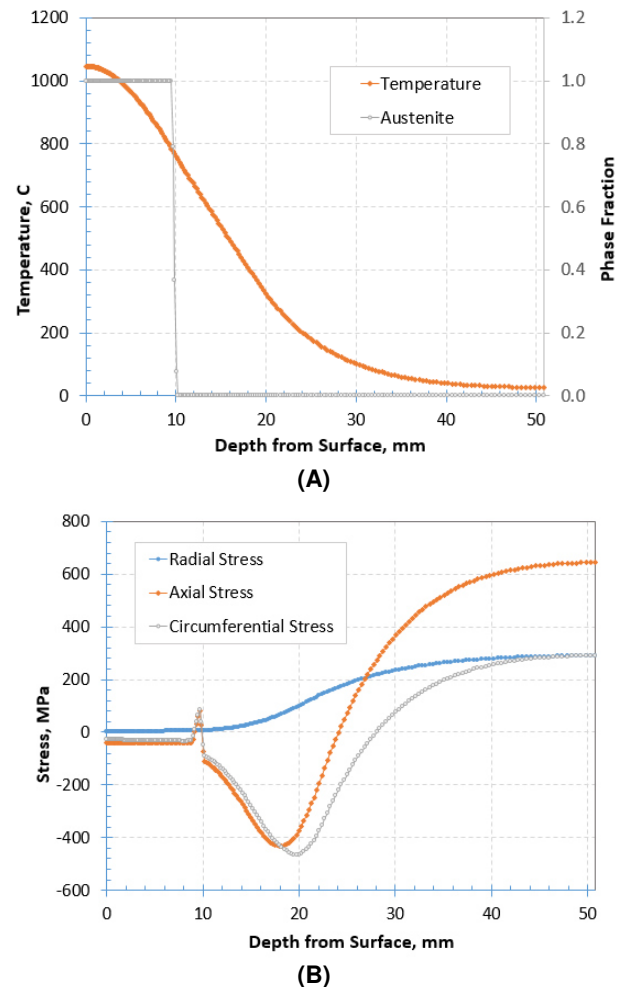


FIGURE 3 – (A) TEMPERATURE AND AUSTENITE, AND (B) STRESS DISTRIBUTION AT THE END OF INDUCTION HEATING.

The predicted highest temperature is 1045° C, located right at the surface. The depth of the austenite layer formed is about 10 mm. At the end of the induction heating, the internal stresses inside a part are higher than those of conventional furnace heating because the temperature distribution after the short induction heating time is not uniform. The austenitized surface layer (about 10 mm) has a low or close to neutral stress, as shown in Figure 3(b). Under the austenite layer, both axial and circumferential stresses are in compression with peak values

about 400 MPa, which is due to the thermal expansion in that region. The core of the cylinder is under tension to balance the stress throughout the cylinder.

After induction heating, the cylinder is spray quenched immediately without a time delay. Compared to a conventional liquid quenching process, the cooling rate of an induction spray hardening process is higher because the core of the part is either not heated or heated to a lower temperature compared to conventional furnace heating, and the heat in the austenite layer is conducted into the core in addition to the surface cooling from spray quenching. Almost the entire austenite layer is transformed to martensite at the end of quenching process, as shown in Figure 4. The predicted residual stresses at the end of the quench are also shown in Figure 4, with the hardened case having compressive axial and circumferential stresses. Under the hardened case with a depth range from 10 mm to about 22 mm, both axial and circumferential stresses are tensile.

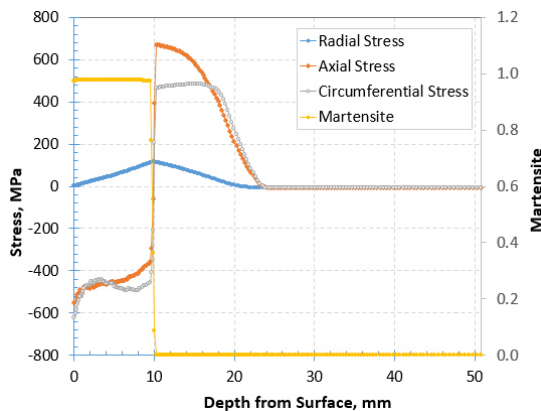


FIGURE 4 – RESIDUAL STRESSES AND MARTENSITE DISTRIBUTIONS AT THE END OF HARDENING.

As mentioned, quench hardening is a highly nonlinear process due to the phase transformation. The phase transformations will cause thermal and mechanical property changes during quenching. Because martensite has a lower density than austenite, the material expands when martensite forms, which leads to localized stresses and plastic deformation. Figure 5 shows the axial stress history at various times during the spray quench. The '0s' line represents the stress distribution right at the end of the induction heating process. The stress magnitude is low in the austenite layer because the thermal gradient in the austenite layer is low, the hot austenite has low yield strength, and because the stress is relaxed while austenite is formed due to the transformation induced plasticity (TRIP) effect. At 3.526 s into the quench, the surface has cooled to a temperature above the martensitic transformation starting temperature (M_s). Without forming martensite, the material thermally contracts, and tensile stresses are generated in the austenite layer, with the highest tensile stress of 300 MPa at the surface. After spray quenching for 5.509 s, the martensitic phase transformation starts at the surface, and the surface stress is shifted from tension to compressive stress due to the volume expansion. With further

cooling, martensite transformation moves deeper from the surface until the entire layer transforms to martensite at about 35 seconds of quenching. The temperature at the core is still warm when the martensitic transformation is completed in the case, and the core is under compression. With further cooling, when the core cools down to room temperature, the thermal shrinkage in the core reduces its compression magnitude, or even shifts to tension depending on the degree of the temperature change. To balance the core stress change, the surface compression will increase. The stress evolution in Figure 5 shows that the final cooling of the core has significant effect on the final residual stresses in the hardened case. The degree of the core thermal shrinkage can be adjusted or designed to enhance the surface compression in the hardened case. The following section in the paper describes an innovative potential process for enhancing the surface compression by increasing the thermal shrinkage effect in the core during the induction hardening process.

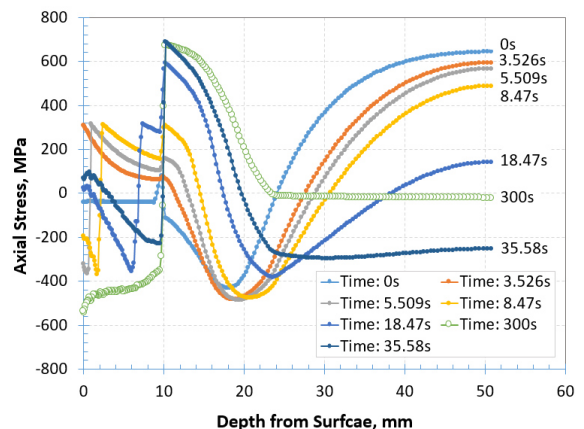


FIGURE 5 – AXIAL STRESS EVOLUTION DURING SPRAY QUENCH AFTER INDUCTION HEATING.

PROCESS IMPROVEMENT TO INCREASE THE SURFACE RESIDUAL STRESS

The modeling results of the single shot induction hardening process have shown that the thermal shrinkage of the core during the later stage of the process is critical to the final magnitude of compressive residual stress in the hardened case. By preheating the parts prior to induction hardening to temperatures below the lower critical temperature, the thermal shrinkage of the core will be more significant, and the surface residual compression will be enhanced. In this section, this concept is modeled and demonstrated by computer modeling of the cylinder using DANTE. Two preheating methods are used: 1) furnace preheating the component to a uniform temperature, and 2) induction preheating using low power and/or low frequency to a non-uniform temperature.

By using furnace preheating, the cylinder is through heated to 150° C, followed by induction hardening with the assumption of no delay between the two processes. The second preheating method uses low power induction heating. In this paper, the power applied during induction preheating is 5% of

the baseline induction heating process, which is 0.125 kW for the 0.5 mm sliced model. The inductor frequency is 3.5 kHz, and it is the same as that used in the baseline model. The total time used for the preheating is 60 s. The temperature distributions in terms of depth from the OD surface are shown in Figure 6 at the end of preheating for both scenarios. By using induction preheating, the surface temperature reaches about 325° C, and the core is slightly higher than 150° C. In both cases the temperatures are well below the lower critical temperature and no phase transformations have occurred.

After preheating, the cylinder is induction hardened immediately without delay. In reality, a transfer time from the furnace to the induction hardening equipment is required if a furnace preheating method is used. The effect of the transfer time (or delay time) between induction preheating and induction hardening can be assessed by modeling, but it is not considered in this paper.

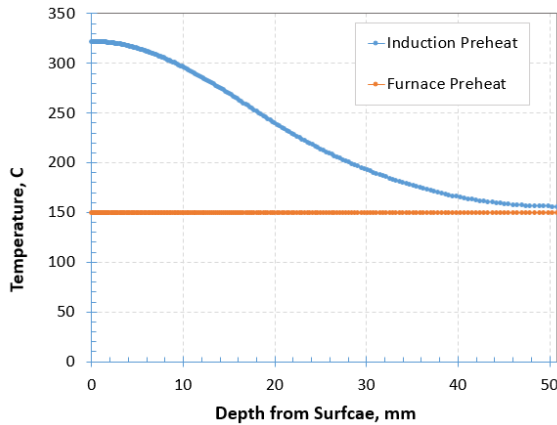


FIGURE 6 – PREHEAT THE PART PRIOR TO INDUCTION HARDENING.

After preheating, the same induction heating power and frequency as those of the baseline process are used to harden the cylinder. The goal of induction heating prior to spray quench is to reach approximately 1050° C at the surface at the end of heating, with an approximate 10 mm austenite depth. However, the heating time duration applied for the two scenarios is different due to their different preheating temperature distributions. The heating times are 6.65 s and 5.5 s for the furnace preheating and the induction preheating scenarios, respectively. The predicted temperature and austenite distributions for the two preheating scenarios are compared with the baseline model in Figure 7. The predicted temperatures at the core are 27° C, 150° C, and 175° C, respectively for the baseline, furnace preheat, and induction preheat models.

The predicted residual stresses in the axial direction are compared in Figure 8(a) for the three scenarios. For the baseline model, the predicted axial compression at the surface is 557 MPa, compared to 693 MPa, and 753 MPa in compression for the furnace preheating and induction preheating scenarios. The surface compressive stress

enhancement is 24.4% and 35% respectively, which is significant to the fatigue performance of the part.

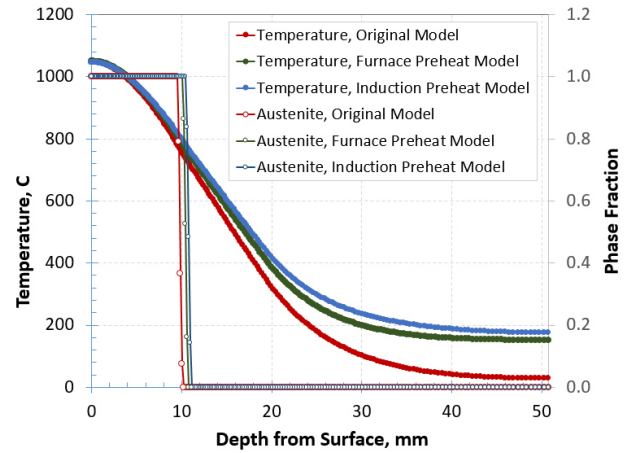


FIGURE 7 – TEMPERATURE AND AUSTENITE DISTRIBUTIONS AT THE END OF INDUCTION HEATING.

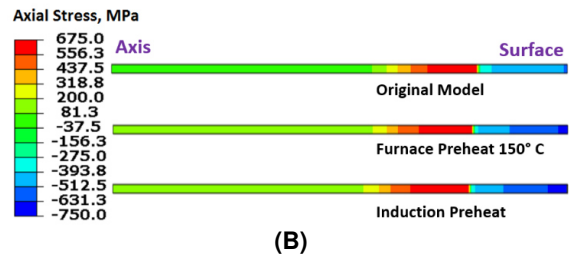
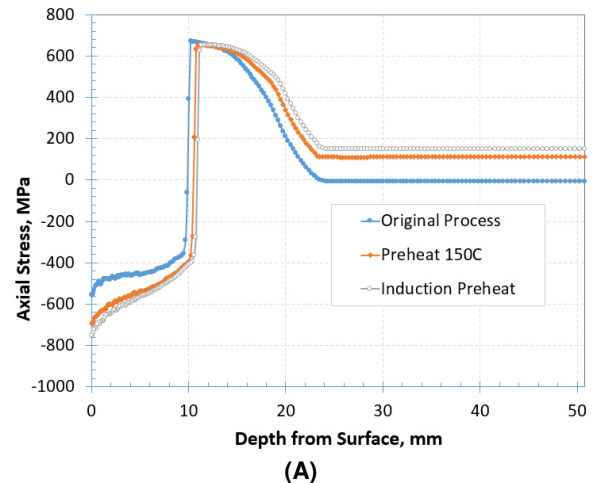


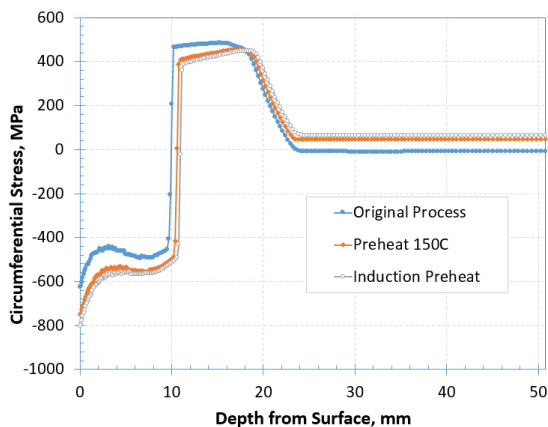
FIGURE 8 – COMPARISON OF AXIAL RESIDUAL STRESSES OF THE THREE (3) MODELS: (A) CURVE PLOTS, AND (B) CONTOUR PLOTS.

Figure 8(b) shows the residual stress distribution contours for the three scenarios. The left side of the contour represents the axis of the cylinder, and the right side is the outer surface. From both the curve plots and the contour distributions, it is clearly seen that the core of the cylinder is under tension for the two preheating scenarios, while the predicted axial stress in the core is neutral for the baseline model. Achieving a tensile

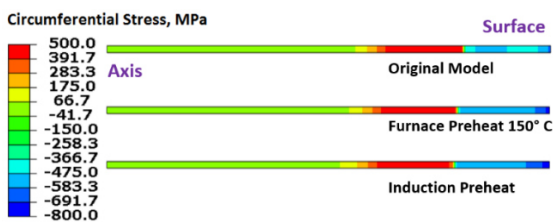
residual stress in the core is therefore the key to enhancing the surface compression. Higher surface compression requires that it be balanced by sub-surface tension. As discussed below, the sub-surface tensile stress is not necessarily detrimental, but it must be taken into account.

It is worth discussing that the residual stresses in the core are not always neutral for induction hardening processes conducted without using preheating. In induction hardening, the tensile residual stresses under the hardened case may initiate high cycle fatigue cracks. In this example, the predicted tensile peak under the case is 670 MPa for the baseline, and the tensile peak decreases slightly to 630 MPa for the preheating scenarios. Also, the location of the tensile peak is at a slightly greater depth from the surface than the peak for the baseline model.

The predicted residual stresses in the circumferential direction are shown in Figure 9. The predicted circumferential residual stresses at the surface are more compressive than the axial stresses, with the preheating also significantly enhancing the compression in the circumferential direction. The residual tension under the hardened case is lower in the circumferential direction than that of that of the axial direction, but it is spread over a wider radial depth.



(A)



(B)

FIGURE 9 – COMPARISON OF CIRCUMFERENTIAL RESIDUAL STRESSES OF THE THREE (3) MODELS: (A) CURVE PLOTS, AND (B) CONTOUR PLOTS.

CONCLUSIONS

The single shot induction hardening process of a cylinder has been modeled using the finite element based software DANTE. The modeling results have explained how residual

stresses are generated during the induction hardening process, with the major effect due to the transformation of austenite to martensite. Preheating the part using a furnace or low power induction can be combined with standard induction hardening to enhance the obtained surface compression in the hardened case, which is critical to the part fatigue performance. The preheating is proven to be significant by the computer modeling, and the preheating can be designed without introducing detrimental residual tension in the critical areas.

FUTURE RESEARCH

In this paper, a simplified disk model is used to represent a cylindrical pin, and the single shot preheat method is applied. To make the process more practical and easier implementation in a heat treat plant. In future works, the preheat using scanning induction heating will be modeled, and the scanning process parameters will be designed, and further experimental validations will also be implemented.

REFERENCES

- [1] Goldstein, R., Nemkov, V., Madeira, R.: Optimizing Axle-Scan Hardening Inductors. *Industrial Heating*, 12, 2007.
- [2] G. Golovin, Residual Stresses and Deformation during High-Frequency Surface Hardening, Mashghiz, Moscow, 1962 (in Russian).
- [3] S. Jahanian. Thermoelastoplastic and Residual Stress Analysis during Induction Hardening of Steel, *Journal of Materials Eng. and Performance*, V. 4, Issue 6, 1995.
- [4] Li, Z., Ferguson, B., Goldstein, G., Nemkov, V., Jackowski, J., and Fett, G.: Modeling Stress and Distortion of Full-float Truck Axle during Induction Hardening Process, 27th ASM-HTS Conference, 2013.
- [5] J. Grum, Overview of residual stresses after induction surface hardening. *International Journal of Materials and Product Technology*, Volume 29, no.1-4, 2007.
- [6] B. Lynn Ferguson, A. Freborg, and G. Petrus, "Software Simulates Quenching", *Advanced Materials and Processes*, H31-H36, August (2000).
- [7] W. R. Schwenk, Simultaneous Dual-Frequency Induction Hardening, *Heat Treating Progress*, 35-38, (April/May 2003).
- [8] W. Dowling, et al., "Development of a Carburizing and Quenching Simulation Tool: Program Overview," 2nd Int. Conference on Quenching and Control of Distortion, eds, G. Totten, et al., ASM Int., 1996.
- [9] Li, Z., Ferguson, B., and Freborg, A., "Data Needs for Modeling Heat Treatment of Steel Parts", *Proceedings of Materials Science & Technology Conference*, 2004, pp. 219-226